

Superconductivity and crystallographic transitions of InBi under pressure

This content has been downloaded from IOPscience. Please scroll down to see the full text.

1998 J. Phys.: Condens. Matter 10 7303

(<http://iopscience.iop.org/0953-8984/10/33/003>)

View [the table of contents for this issue](#), or go to the [journal homepage](#) for more

Download details:

IP Address: 131.170.6.51

This content was downloaded on 24/08/2014 at 21:43

Please note that [terms and conditions apply](#).

Superconductivity and crystallographic transitions of InBi under pressure

V G Tissen[†], V F Degtyareva[†], M V Nefedova[†], E G Ponyatovskii[†] and
W B Holzapfel^{‡§}

[†] Institute of Solid State Physics, Russian Academy of Sciences, 142432 Chernogolovka,
Moscow district, Russia

[‡] FB 6 Physik, Universität-GH-Paderborn, 33095 Paderborn, Germany

Received 2 April 1998, in final form 12 May 1998

Abstract. Measurements of the superconducting transition temperature T_c of the compound InBi under pressures up to 40 GPa reveal three different regions corresponding to the observed structural transitions I–II–III from the initial phase I of InBi type (*tP4*) to phase II of β -Nb type (*tP4*) and to a *body-centred tetragonal* phase III (*tI2*). Some similarities and distinct differences in the superconducting and structural behaviour of the III–V compound InBi in comparison with the isoelectronic group IV element Sn point to some differences in the possible mechanisms for the crystallographic transformations under pressure.

1. Introduction

Group IV elements and isoelectronic III–V compounds are intensively studied experimentally and theoretically because of the semiconductor-to-metal transition observed on moving from lighter to heavier elements as well by increase of pressure. The lighter group IV elements Si and Ge transform under pressure from a *diamond* type (*cF8*) semiconducting structure to *metallic* phases of *white tin* type (*tI4*) and *simple hexagonal* (*hP1*) structure [1, 2]. III–V compounds with *diamond*-like structures of *zinc blende* or *wurtzite* type at ambient pressure have high-pressure forms based on *NaCl* type, *white tin* type or *simple hexagonal* structures with additional complexities such as orthorhombic distortions and superlattices with or without effects of atomic ordering.

The heavier group IV element Sn does not transform under pressure to the *simple hexagonal* structure but shows the different structural sequence [3]: *grey tin* (*cF8*) \rightarrow *white tin* (*tI4*) \rightarrow *tetragonal body centred* (*tI2*) \rightarrow *cubic body centred* (*cI2*). Some similarity with this behaviour was observed recently in a high-pressure study on the heavier III–V compound InBi [4]. Unlike the lighter III–V compounds, which are semiconductors at ambient conditions, InBi forms a semimetallic compound with tetragonal structure of its own type, *tP4*, space group *P4/nmm* with In in the special position 2a ($000; \frac{1}{2} \frac{1}{2} 0$) and Bi in 2c ($0 \frac{1}{2} z; \frac{1}{2} 0 \bar{z}$) with $z = 0.393$ [5]. InBi is not superconducting at ambient pressure above 0.5 K [6].

Structural transformations of InBi under pressure are expected to affect also other physical properties. Especially, the behaviour of the superconducting transition temperature,

§ E-mail address for correspondence: holz_we@physik.uni-paderborn.de.

T_c , in this compound seems to be interesting in comparison with high pressure studies of superconductivity in Sn [7–9] from the point of view that some correlations between crystal structures and superconducting properties of high-pressure phases had been established earlier [10] showing a trend of increase in T_c with increasing packing density.

2. Experiment

The sample material was obtained by melting stoichiometric amounts of the pure elements (99.99%) in evacuated silica tubes with further thermobaric treatment as described previously [11]. The structural studies were performed with diamond anvil cells [12] and energy dispersive x-ray diffraction using synchrotron radiation at the beamline F3 of HASYLAB/DESY [13,14]. Either standard diamond anvils with flat faces of 600 μm or bevelled faces of 300 μm diameter were used depending on the required maximum pressure. The samples were mounted in the gasket hole of 100–200 μm diameter together with ruby or gold as a pressure marker and mineral oil as pressure transmitting medium. All the diffraction patterns are obtained at ambient temperature; however in one series the sample was heated at ~ 17 GPa up to 240 $^\circ\text{C}$ for 1 hour to reduce deviatoric stresses before the measurements were performed. More details of the structural studies are described elsewhere [4]. Specially adopted software [15] was used for the evaluation of the diffraction spectra.

A diamond anvil cell made out of a nonmagnetic alloy was used in the high-pressure study of the superconducting transition temperature on samples with typical dimensions of $80 \times 80 \times 30 \mu\text{m}^3$. Anvils with 500 μm culet diameter were mounted in this case on sapphire backing plates in order to decrease the inductive coupling between the metallic surroundings and the coil system used for the ac susceptibility measurements. Gaskets were preindented to 60 μm from an initial thickness of 300 μm . The sample and several small ruby chips were loaded in the gasket hole of 150 μm diameter. The common methanol–ethanol mixture in the ratio 4:1 served as pressure transmitting medium. The cell was cooled down to 1.4 K in a liquid He cryostat. The temperature was measured by a Cu–Fe/Cu thermocouple with an accuracy of ± 0.2 K. The pressure was determined at room temperature by the ruby fluorescence method using the nonlinear ruby scale [16] without any correction for thermal-pressure shifts. The superconducting transition was detected by measuring the ac magnetic susceptibility as a function of temperature during the heating cycle, thereby the pick-up coil was positioned around the anvils and a reference coil was placed nearby. The two coils were parts of an inductor bridge. After initial compensation the signal was detected with a lock-in amplifier. All the other details of this methods have been described just previously [17].

3. Results and discussion

Since the structures of the high-pressure phases InBi(II) and InBi(III) were determined just recently [4], the structural transitions of InBi will be discussed here only with respect to results on T_c of InBi under pressure.

As illustrated in figure 1, diffraction patterns of InBi show two transformations with increasing pressure, one at ~ 7 GPa and one at ~ 20 GPa. The crystal structure of InBi(II) is tetragonal with four atoms in the unit cell, $tP4$, space group $P4/nmm$. It is isostructural with InBi(I), but with strong compression along the c -axis to $c/a \approx 0.60$. Therefore, the structure shows some similarity to β -Nb, however, with its two different atomic species in

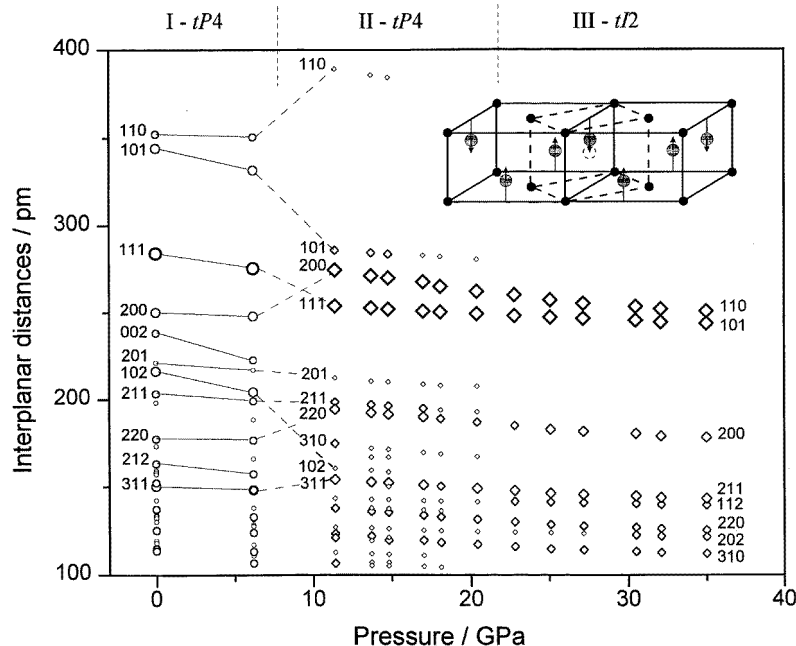


Figure 1. d_{hkl} -values for InBi under pressure. Only two sets of data are shown for phase I and data with phase mixture in the transition region from phase I to phase II are also omitted for clarity. Indices for the $tP4$ structure are given for both the phases I and II for the stronger peaks. Phase III is indexed according to a $tI2$ structure. The inset illustrates structural relations for the InBi(II)–(III) transition. Solid lines represent the structure of InBi(II, $tP4$) with In in the position $2a$ ($000; \frac{1}{2}\frac{1}{2}0$) and Bi in $2c$ ($0\frac{1}{2}z; \frac{1}{2}0\bar{z}$). At the transition to InBi(III, $tI2$) z increases to $\frac{1}{2}$ reducing the cell to $tI2$ (dashed lines) with disordering of the atoms.

the two different positions: In in $2a$ ($000, \frac{1}{2}\frac{1}{2}0$) and Bi in $2c$ ($0\frac{1}{2}z, \frac{1}{2}0\bar{z}$). This structure, InBi(II), shows ‘compositional order’ (see inset to figure 1). The value of the parameter z is determined from the intensity ratio of the (211) and (220) peaks, since this intensity ratio is very sensitive to the value of z . As can be seen in figure 2, this small section of the diffraction spectra demonstrates that the intensity of the (211) peak decreases with increasing pressure. The free atomic parameter z for Bi changes from $z = 0.326$ at 3.1 GPa (observed on decompression) to $z = 0.5$ at pressures above 20 GPa. At $z = 0.5$ the structure changes to higher symmetry and can be described with a smaller unit cell containing only two atoms. InBi(III) must be compositionally disordered, because no superstructure peaks for atomic ordering in a primitive tetragonal cell ($tP2$) are observed. Therefore the structure of InBi(III) is considered to be body-centred tetragonal ($tI2$) space group $I4/mmm$.

The structural transformation II–III seems to be continuous, as shown in figures 1 and 2. The c/a -ratio as function of pressure is shown in figure 3(a) for all the three phases to illustrate the discontinuity at the I–II transition and the continuous changes in the II–III transition, whereby the $tP4$ assignment is used in this case also for InBi(III).

At ambient pressure, no T_c was observed in InBi above 1.4 K in accordance with the previous work [6]. However, the small increase in pressure to 0.8 GPa results in a noticeable superconducting signal which indicates that T_c is close to 1.4 K in this case. The width

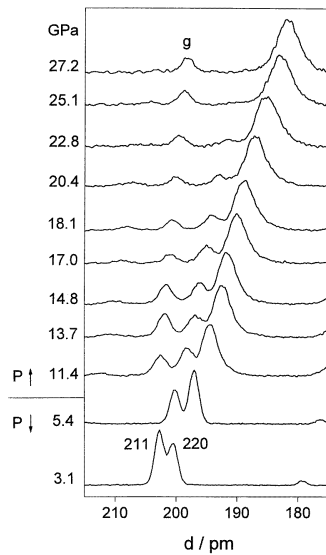


Figure 2. Sections of energy dispersive x-ray diffraction spectra for InBi under pressure, including the two principal peaks (211) and (220) of the $IP4$ structure. 'g' represents a peak from the gasket (inconel) in the spectra taken with $\Theta = 4.943^\circ$. Patterns at 5.4 GPa and 3.1 GPa were obtained on decompression in another run without diffraction from the gasket with $\Theta = 4.850^\circ$ to illustrate the continuous decrease in the relative intensity of the (211) peak in the whole range of pressures.

of the transition is about 0.2 K and does not change appreciably with increasing pressure. The pressure dependence of the superconducting transition temperature T_c (the midpoint of the susceptibility change) is displayed in figure 3(b), which demonstrates a quite different $T_c(P)$ behaviour in three different regions. At first, T_c increases steeply with increasing pressure to about 6 GPa, then $T_c(P)$ has only a small positive slope and above 15 GPa T_c shows a strong decrease.

The pressures values for the anomalies in T_c are close to values where structural transitions occur at room temperature. The small differences can be accounted for by variations of the phase boundaries with temperature and by small differences between the pressures measured at ambient temperature and the actual pressures at low temperature. In any case, the three different regions on the $T_c(P)$ curve are clearly related to the three different structures of InBi (I to III).

The drastic increase of T_c under pressure for InBi(I) represents an unusual behaviour in comparison with normal metals but it correlates with the strong anisotropy of this structure: the compressibility along c is an order of magnitude larger than along a , as shown also earlier by precise measurements with neutron powder diffraction up to 2.6 GPa [18] and confirmed by the recent high pressure x-ray study [4]. At $P = 6.2$ GPa the phase InBi(I) has the lattice parameters $a = 495.1$ pm and $c = 445.7$ pm with $c/a = 0.900$ and extrapolation of the data for phase II down to this pressure gives the lattice parameters $a = 557.7$ pm and $c = 335.4$ pm with $c/a = 0.601$. At the I–II transition the axial ratio decreases thus by 33%, the c -axis decreases by 25%, the a -axis expands by 12.5% and the volume changes by 2%. The sharp increase of T_c with pressure and the elastic anisotropy of InBi(I) correlate with previously observed anomalies in resistivity and acoustic measurements, and had been assigned to pressure induced electron changes [19].

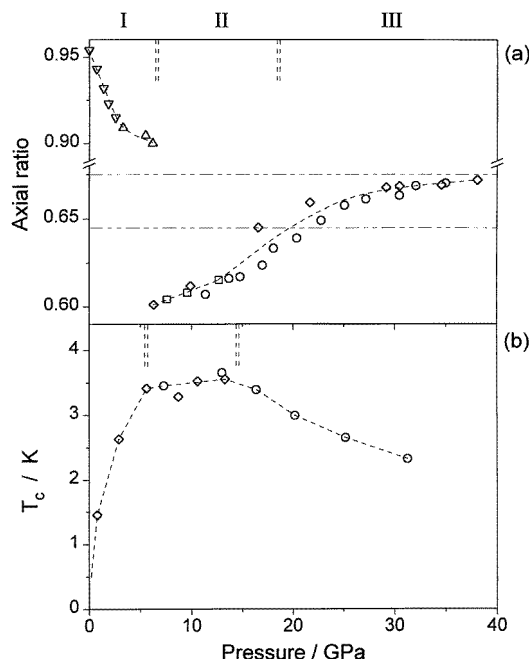


Figure 3. Effect of pressure on InBi illustrating the boundaries between the phases I, II and III: (a) c/a -ratio for a common $tP4$ unit cell (∇ from [17], other symbols—different runs from [4]). Horizontal lines show lower and upper limits of c/a for phase III which are 0.644 and 0.675 for the $tP4$ unit cell and 0.911 and 0.955 for the $tI2$ unit cell, respectively, as discussed in [4]. (b) Superconducting transition temperature T_c (two different runs). Dashed lines are guides to the eye.

It is interesting to compare the structural and superconducting behaviour under pressure for InBi with the isoelectronic group IV element Sn. The structural analogue of β -Sn($tI4$) is the β -Np-like structure of InBi(II, $tP4$) because both structures are tetragonal with four atoms in the unit cell and show nearly the same axial ratios. While the β -Sn structure has space group $I4_1/amd$ with one atomic position 4a ($000, 0\frac{1}{2}\frac{1}{4}$) which accommodates only one atomic species, the β -Np-type structure with space group $P4/nmm$ has two different atomic positions to accommodate two different atomic species. Despite some resemblance of the two structures, the behaviour of T_c for InBi(II) differs considerably from the one of β -Sn, which shows a large decrease of T_c with increasing pressure [7, 8]. Furthermore, the transformation to the Sn($tI2$) structure is accompanied with a discontinuous increase of T_c (figure 4), whereas the II–III transformation of InBi can be described as displacive type with a continuous increase in the atomic parameter z from ~ 0.33 to 0.5. At the value $z = \frac{1}{2}$, the symmetry changes from $P4/nmm$ to $P4/mmm$ (if ordered) or to $I4/mmm$ (if disordered). The absence of any discontinuous change in T_c at the II–III transition is compatible with a (second order) displacive character for this transition. In addition, this transformation seems to involve a change from atomic order to disorder due to a systematic absence of the respective x-ray diffraction intensities for InBi(III). Therefore, InBi(III) is an analogue of bct-Sn($tI2$) and this is a second example of a tetragonally distorted *body-centred* structure with an axial ratio in the range 0.91–0.96. Obviously, this similarity of the pressure dependence of T_c for both InBi(III) and bct-Sn, as shown in figure 4, points also to a close similarity in the electronic structure of both phases.

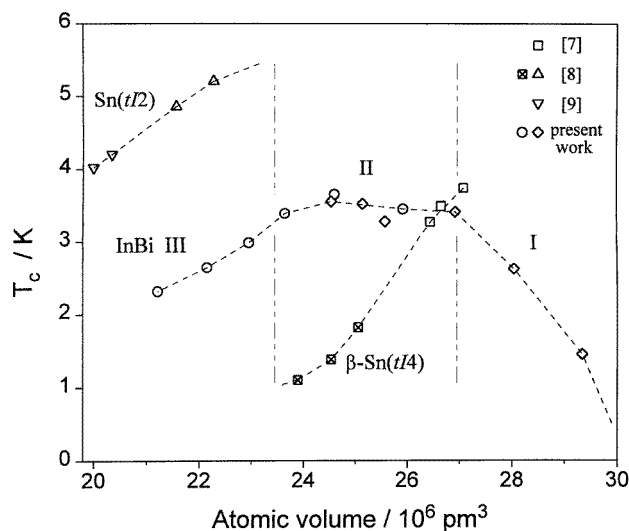


Figure 4. Dependence of T_c on atomic volume for InBi and for Sn. Dashed lines are guides to the eye. Comparison of T_c against volume shows similarities for β -Sn and InBi(II)- β -Np type at the lowest pressure (at nearly equal volumes), but significant difference in T_c behaviour on compression. Further similarities can be noticed in the slopes of $T_c(V)$ for the $tI2$ phases of both substances.

Acknowledgments

The authors wish to thank W Sievers and W Bröckling for experimental assistance. This work was partially supported by the Russian Foundation for Basic Research through grants 96-15-96806 and 96-62-18545.

References

- [1] Sikka S K, Olijnyk H and Holzapfel W B 1984 *Phys. Lett.* **103A** 137
- [2] Vohra Y K, Brister E, Desgreniers S, Ruoff A L, Chang K L and Cohen M L 1986 *Phys. Rev. Lett.* **56** 1944
- [3] Olijnyk H and Holzapfel W B 1984 *J. Physique. Coll.* **45** C8 153
- [4] Degtyareva V F, Winzenick M and Holzapfel W B 1998 *Phys. Rev. B* **57** 4975
- [5] Villars P and Calvert L D 1985 *Pearson's Handbook of Crystallographic Data for Intermetallic Phases* (Materials Park, OH: American Society for Metals)
- [6] Hutcherson J V, Guay R L and Herold J S 1966 *J. Less-Common Met.* **11** 296
- [7] Jennings L D and Swenson C A 1958 *Phys. Rev.* **112** 31
- [8] Wittig J 1966 *Z. Phys.* **195** 215
- [9] Brandt N B and Berman I V 1968 *Zh. Eksp. Teor. Fiz.* **7** 198 (Engl. Transl. *JETP Lett.* **7** 152)
- [10] Ponyatovskii E G and Degtyareva V F 1989 *High Pressure Res.* **1** 163
- [11] Degtyareva V F, Ivakhnenko S A, Ponyatovskii E G and Rashchupkin V I 1982 *Fiz. Tverd. Tela* **24** 1360 (Engl. Transl. *Sov. Phys.-Solid State* **24** 770)
- [12] Syassen K and Holzapfel W B 1975 *Europhys. Conf. Abstr.* **1A** 75
- [13] Grosshans W A, Düsing E F and Holzapfel W B 1984 *High Temp.-High Pressure* **16** 539
- [14] Otto J W 1997 *Nucl. Instrum. Methods A* **384** 552
- [15] Porsch F 1996 *EDX Powder* programme for evaluation of EDXD spectra, RTI, Paderborn
- [16] Mao H K, Bell P M, Shaner J W and Steinberg D J 1978 *J. Appl. Phys.* **49** 32
- [17] Tissen V G, Ponjatovskii E G, Nefedov M V, Porsch F and Holzapfel W B 1996 *Phys. Rev. B* **53** 8238
- [18] Jorgensen J D and Clark J B 1980 *Phys. Rev. B* **22** 6149
- [19] Schirber J E and Van Dyke J P 1977 *Phys. Rev. B* **15** 890